Supplement of Earth Surf. Dynam., 13, 417–435, 2025
https://doi.org/10.5194/esurf-13-417-2025-supplement

Earth Surface Dynamics
Open Access
EGU

Supplement of

Short communication: Multiscale topographic complexity analysis with pyTopoComplexity

Larry Syu-Heng Lai et al.

Correspondence to: Larry Syu-Heng Lai (larrysyuhenglai@gmail.com)

Dated landslides (C^{14} ages)	This study ($\lambda = 15$ m) C value	Booth et al. (2017) ($\lambda \approx 14.535$ m) C^2 value
1 Oso (2±1 yrs BP)	0.03184 m^{-1}	0.001900 m^{-2}
2 Skaglund Hill (230±40 yrs BP)	0.01960 m^{-1}	0.000743 m^{-2}
3 Unnamed-29 (518±40 yrs BP)	0.02546 m^{-1}	0.001108 m^{-2}
4 Rowan (580±40 yrs BP)	0.01941 m^{-1}	0.000786 m^{-2}
5 Unnamed-24 (1243±40 yrs BP)	0.01503 m^{-1}	0.000517 m^{-2}
6 Headache Creek (6017.5±40 yrs BP)	0.01426 m^{-1}	0.000463 m^{-2}
7 Unamed-55 (11692±40 yrs BP)	0.00959 m^{-1}	0.000194 m^{-2}

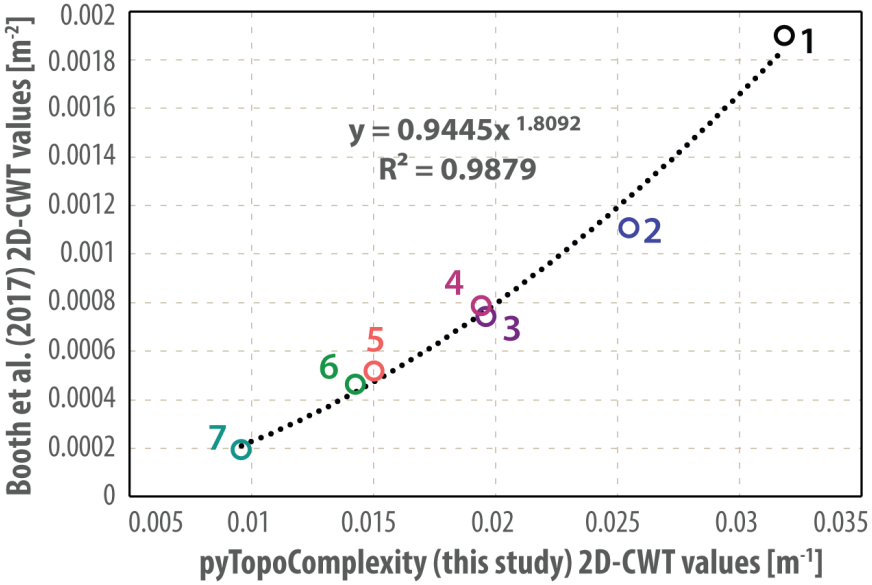

Figure S1: Linear correlation between the two-dimensional continuous wavelet transform (2D-CWT) results obtained in this study and those reported by Booth et al. (2017) for the same dated landslide inventory of the North Fork Stillaguamish River valley (**Fig. 3**), using the newer methods adapted in the pyTopoComplexity (**Eq. 1** and **Eq. 2**) and the older method by Booth et al. (2009), respectively.

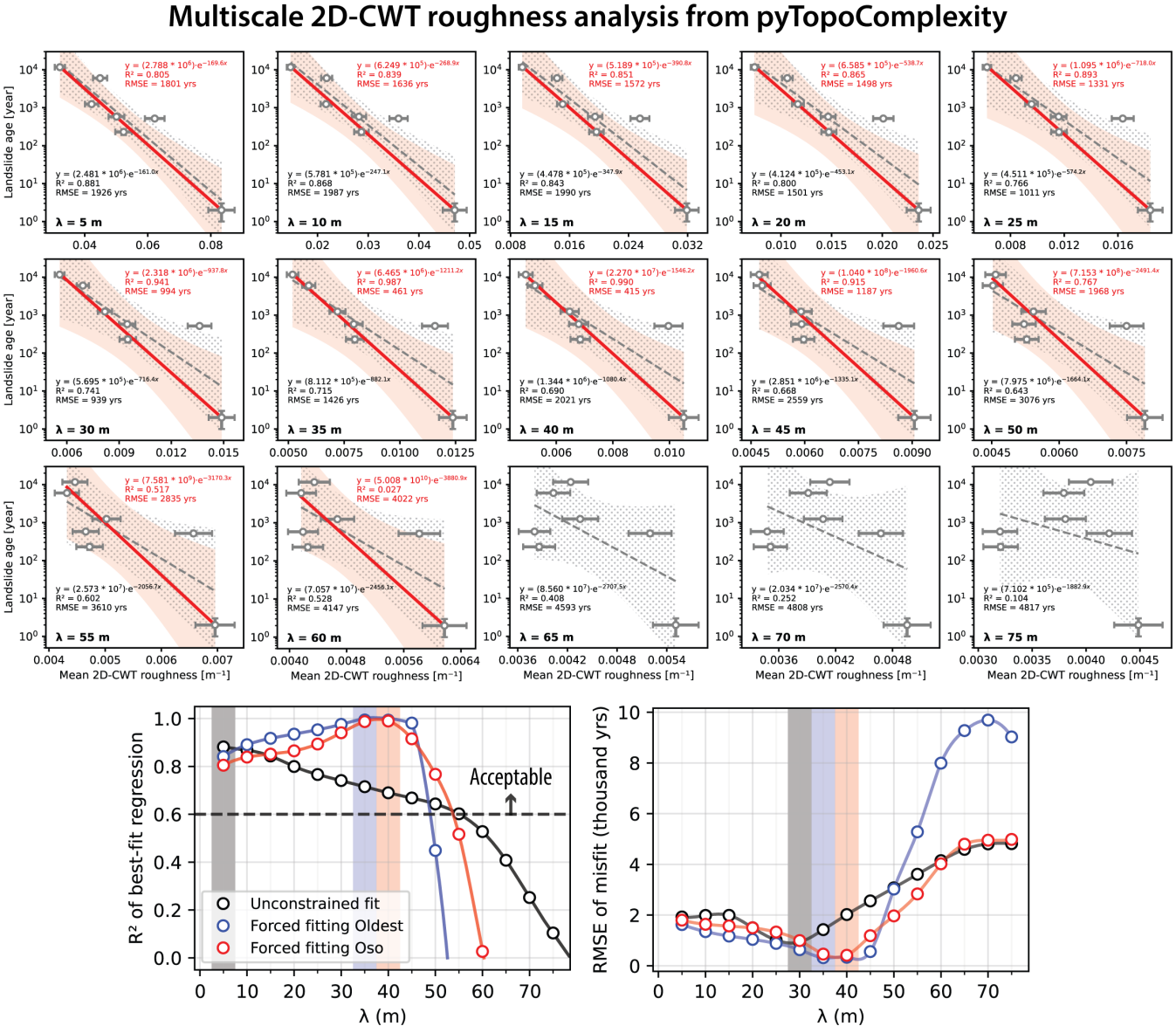

Figure S2: Evaluation of the two-dimensional continuous wavelet transform (2D-CWT) (Booth et al., 2009; Berti et al., 2013) for estimating the age of landslide deposits based on surface complexity, utilizing data from the North Fork Stillaguamish River valley with radiocarbon ages in Booth et al. (2017) (**Fig. 3** and **Fig. S1**). This analysis employed the *pycwtmexhat.py* module from pyTopoComplexity. The spatial scale evaluated (i.e., the Fourier wavelength (λ) of the Mexican hat wavelet) ranges from 5 to 75 meters. The gray dashed lines and shading represent the best-fit exponential decay function and its 95% confidence interval for the seven dated landslides. Red lines and shading indicate the best-fit function constrained to pass through the youngest landslide data point (the 2014 'Oso' landslide). The bottom plots display the coefficient of determination (R^2) and root-mean-square error (RMSE) between radiocarbon age data and the predicted functions. Best-fit curves are excluded if forced fitting yields negative R^2 values. The blue curves represent results for best-fit exponential decay functions constrained to pass through the oldest landslide data point (the 'unnamed-55' landslide). Shaded bars indicate the optimal spatial scale for estimating the surface roughness age of landslide deposits using this method. Only functions with $R^2 > 0.7$ and low RMSE are considered acceptable for estimating the age of landslide deposits.

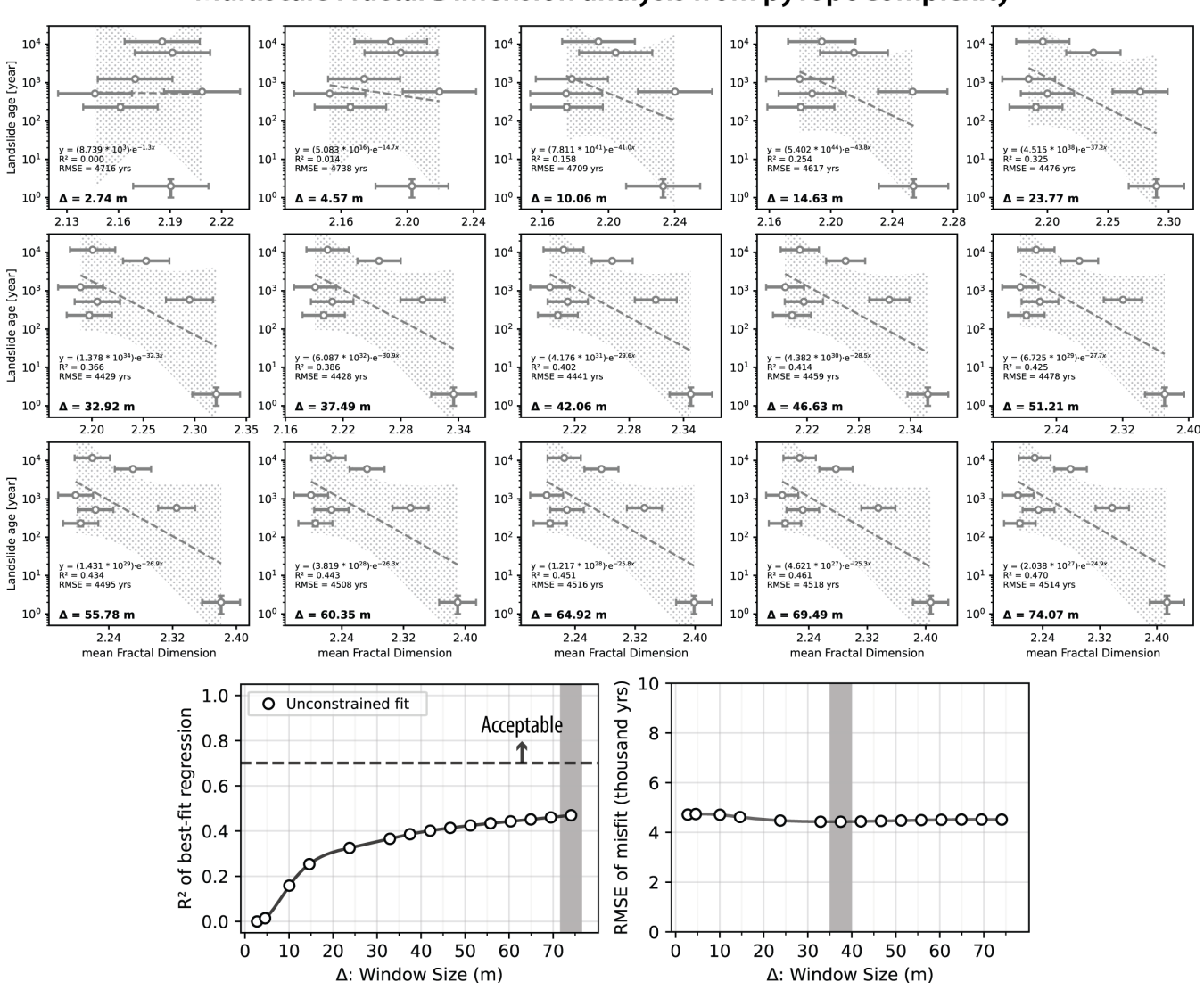

Figure S3: Evaluation of the Fractal Dimension (Wen and Sinding-Larsen, 1997; Pardo-Igúzquiza and Dowd, 2020) for age of landslide deposits based on surface complexity, utilizing data from Booth et al. (2017) (**Fig. 3** and **Fig. S1**). This analysis utilized the pyfracd.py module of pyTopoComplexity. The evaluated spatial scale (window size Δ) ranges from 3 to 81 grids, corresponding to 9 feet (~2.74 m) to 243 feet (~74.07 m) with an input digital terrain model (DTM) featuring 3 feet (~0.9144 m) grid spacing. Other captions follow **Fig. S2**.

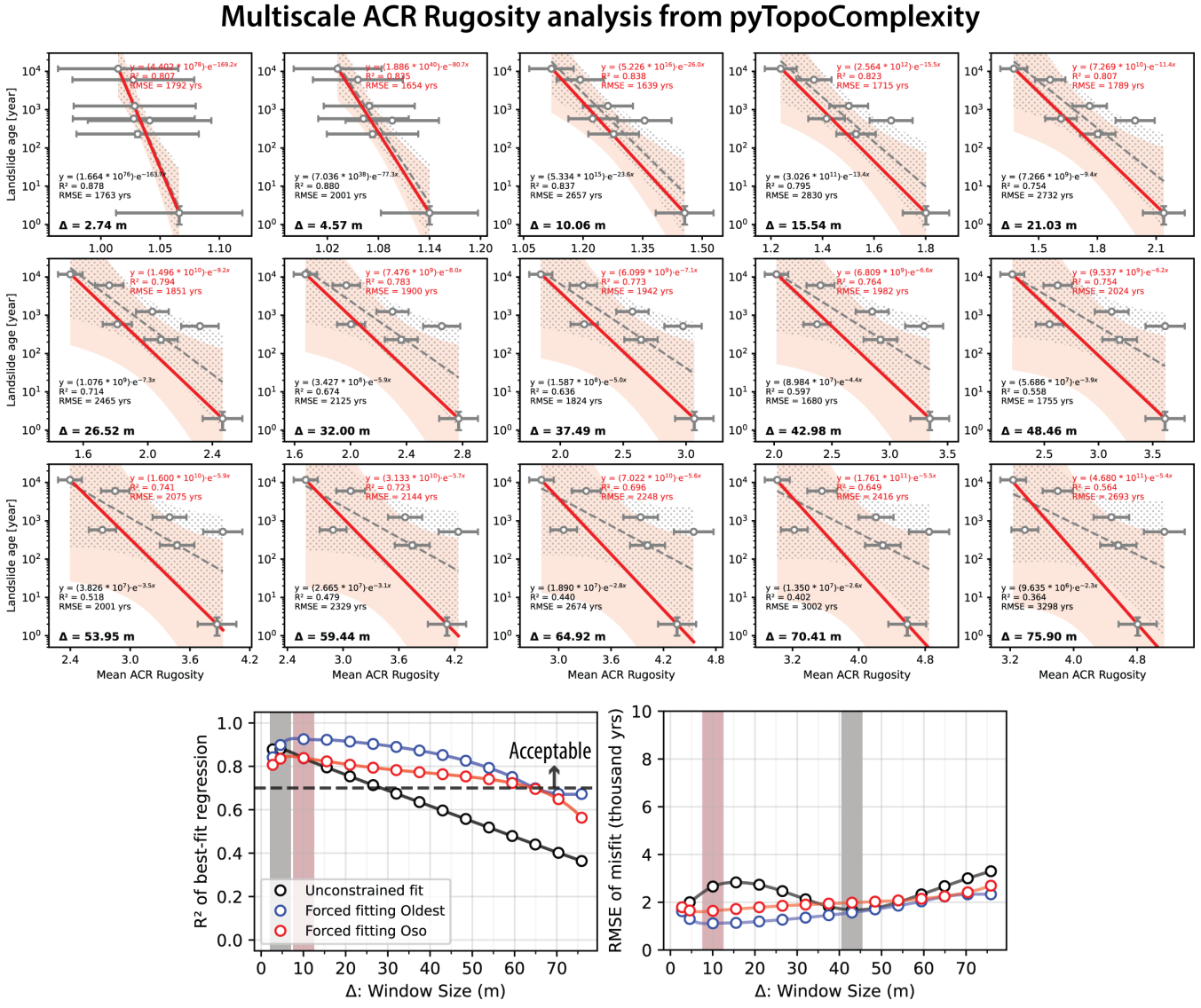

Figure S4: Evaluation of the arc-chord ratio (ACR) Rugosity Index (Du Preez, 2015) for age of landslide deposits based on surface complexity, utilizing data from Booth et al. (2017) (**Fig. 3** and **Fig. S1**). This analysis utilized the pyrugosity.py module of pyTopoComplexity. The evaluated spatial scale (window size Δ) ranges from 3 to 83 grids, corresponding to 9 feet (~2.74 m) to 249 feet (~75.90 m) with an input DTM featuring 3 feet (~0.9144 m) grid spacing. Other captions follow **Fig. S2**.

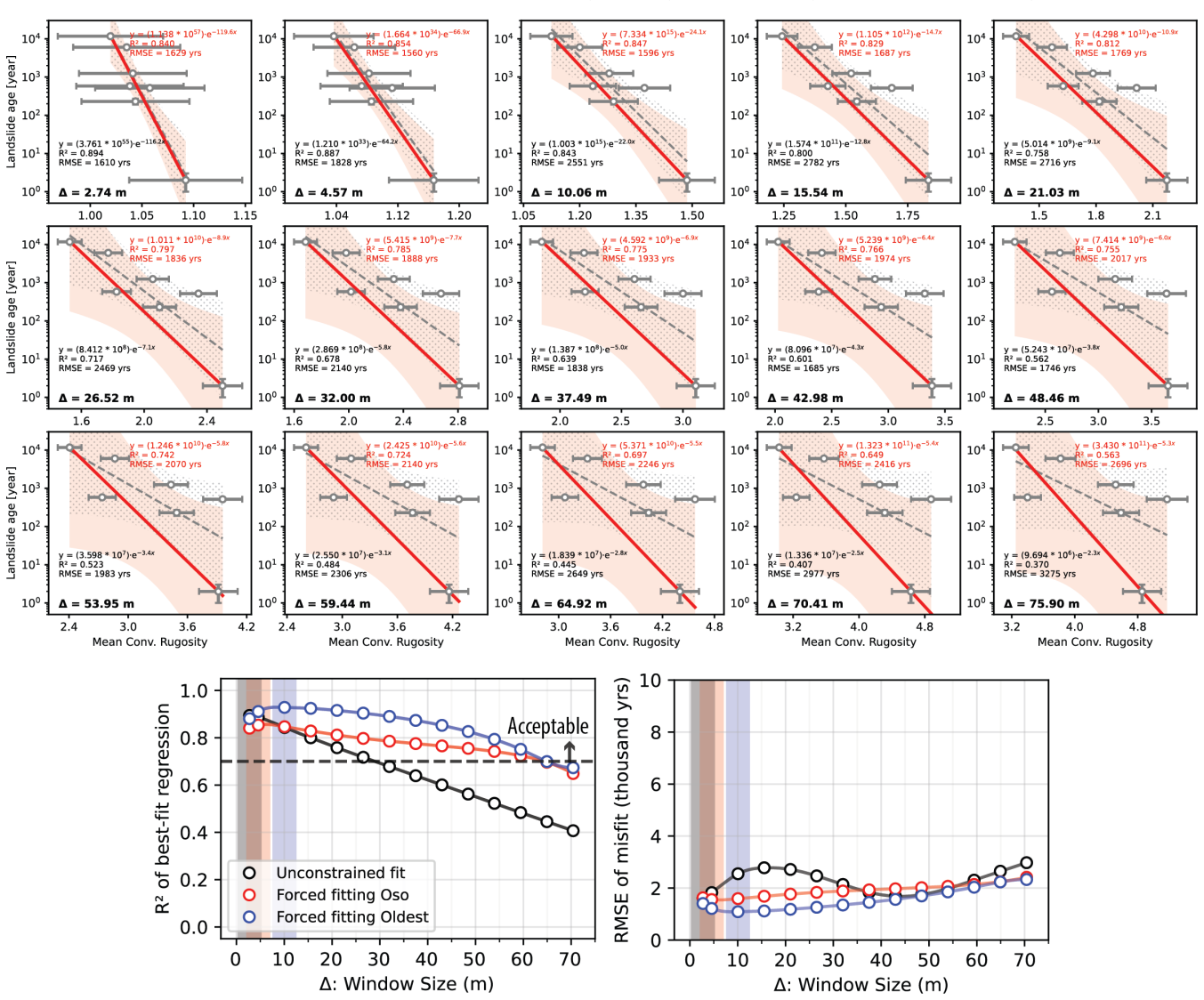

Figure S5: Evaluation of the conventional Rugosity Index (Jenness, 2004) for age of landslide deposits based on surface complexity, utilizing data from Booth et al. (2017) (**Fig. 3** and **Fig. S1**). This analysis utilized the pyrugosity.py module of pyTopoComplexity. The evaluated spatial scale (window size Δ) ranges from 3 to 83 grids, corresponding to 9 feet (~2.74 m) to 249 feet (~75.90 m) with an input DTM featuring 3 feet (~0.9144 m) grid spacing. Other captions follow **Fig. S2**.

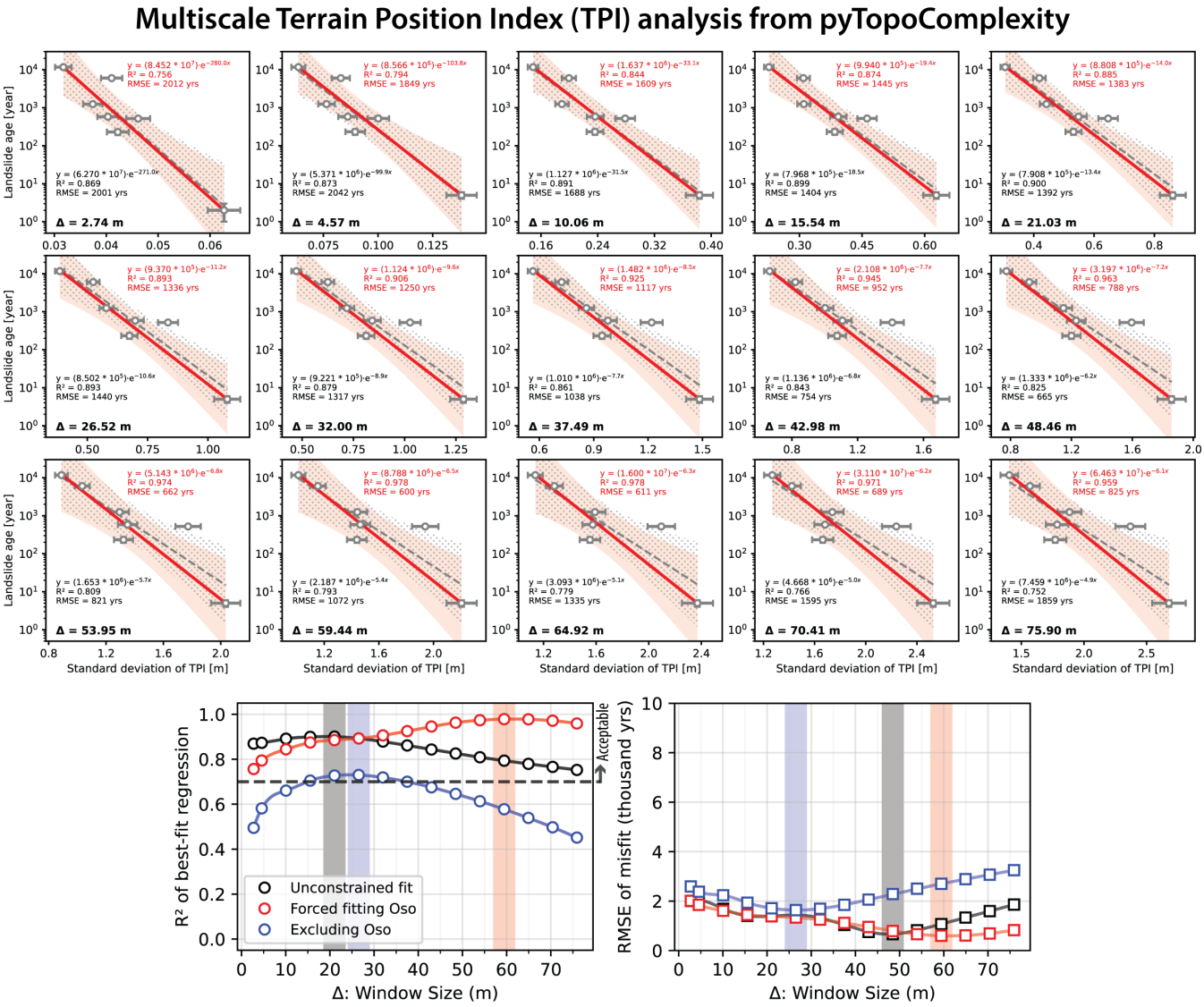

40 **Figure S6:** Evaluation of the Terrain Position Index (Weiss, 2001) for age of landslide deposits based on surface complexity, utilizing data from Booth et al. (2017) (**Fig. 3** and **Fig. S1**). This analysis utilized the pytpi.py module of pyTopoComplexity. The evaluated spatial scale (window size Δ) ranges from 3 to 83 grids, corresponding to 9 feet (~2.74 m) to 249 feet (~75.90 m) with an input digital terrain model featuring 3 feet (~0.9144 m) grid spacing. Other captions follow **Fig. S2**.

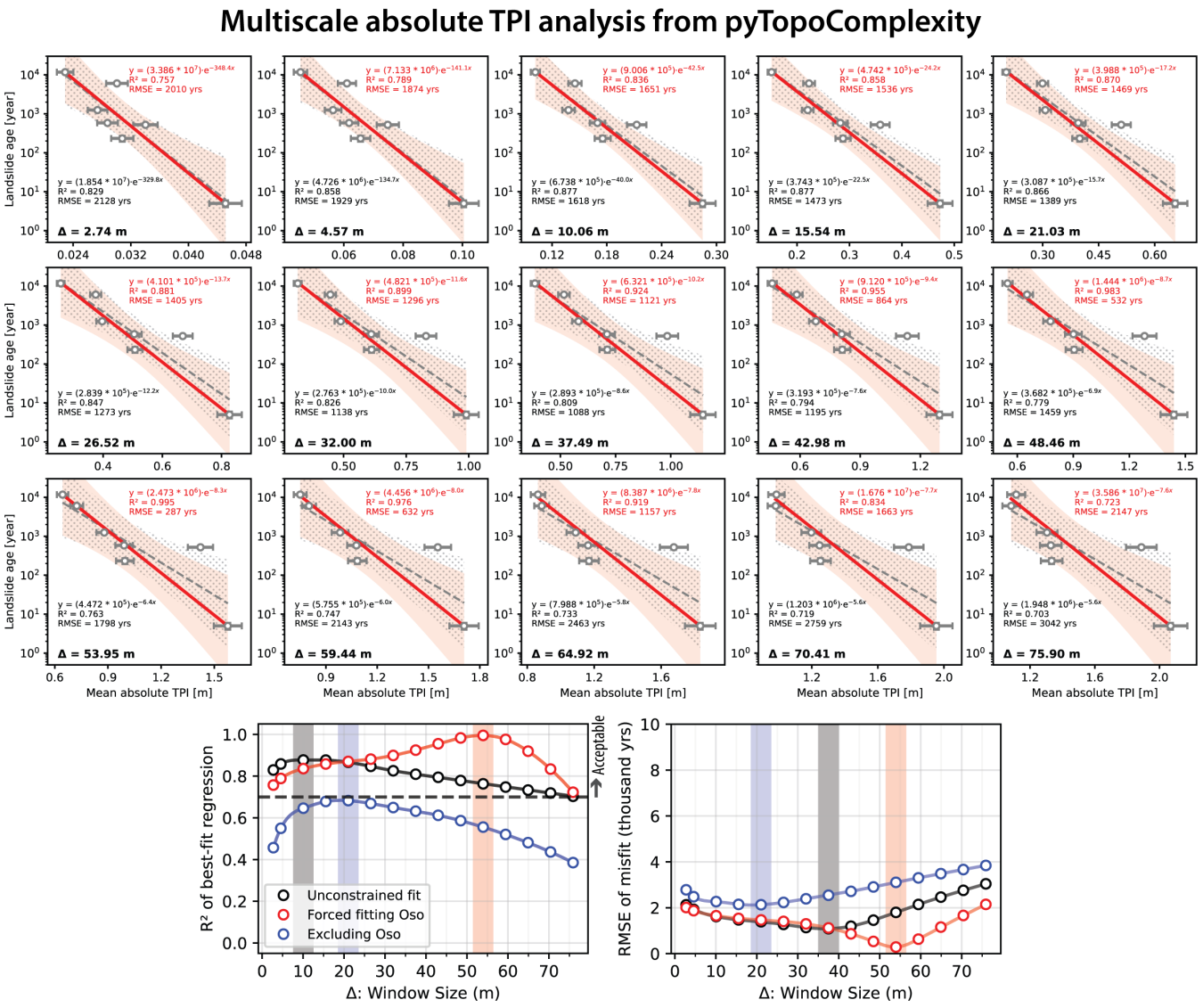

Figure S7: Evaluation of the absolute value of Terrain Position Index (Weiss, 2001) for age of landslide deposits based on surface complexity, utilizing data from Booth et al. (2017) (**Fig. 3** and **Fig. S1**). This analysis utilized the pytpi.py module of pyTopoComplexity. The evaluated spatial scale (window size Δ) ranges from 3 to 83 grids, corresponding to 9 feet (~2.74 m) to 249 feet (~75.90 m) with an input digital terrain model featuring 3 feet (~0.9144 m) grid spacing. Other captions follow **Fig. S2**.

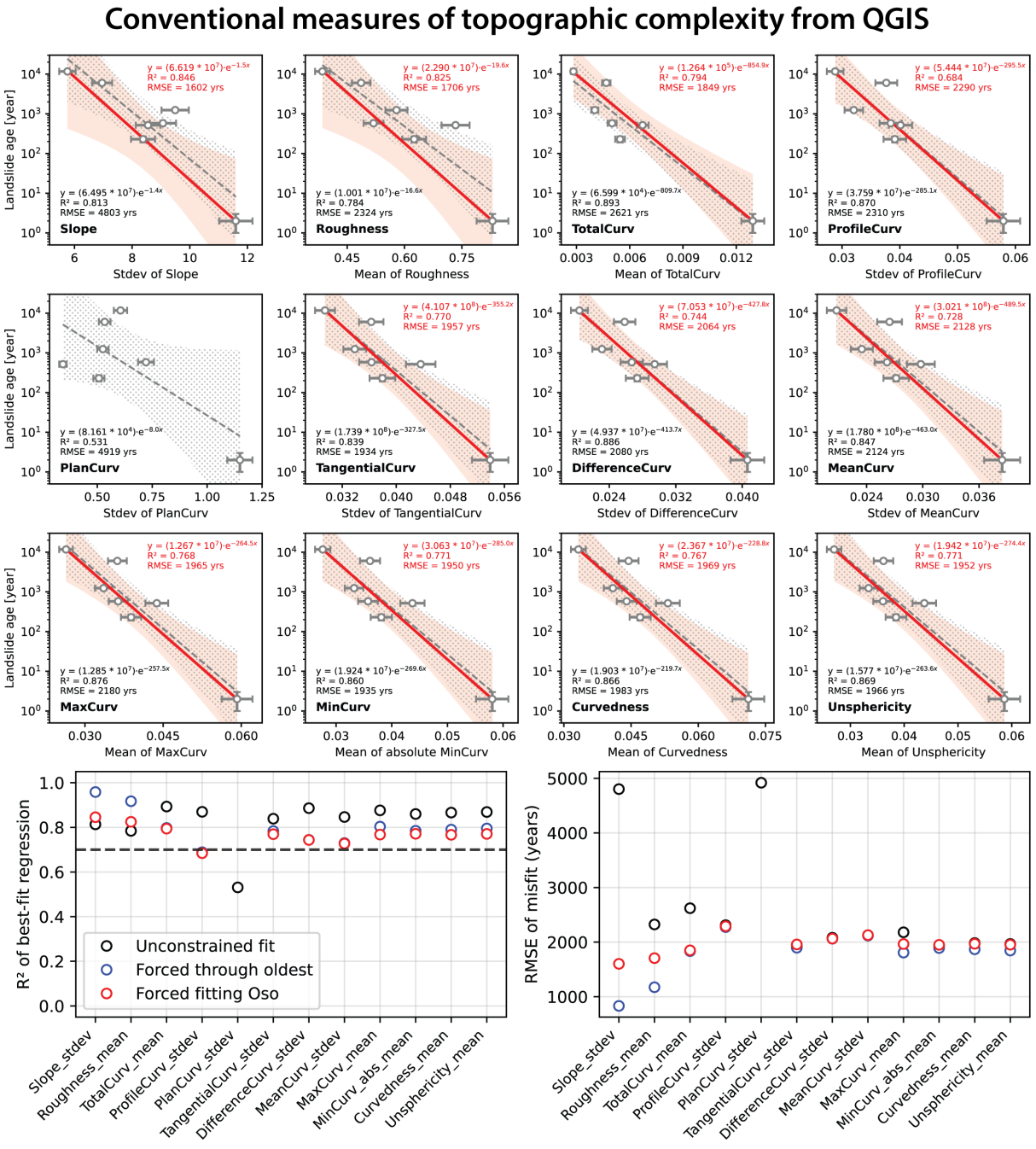

Figure S8: Evaluation of conventional topographic complexity metrics for age of landslide deposits based on surface complexity, utilizing data from Booth et al. (2017) (**Fig. 3** and **Fig. S1**). This analysis was conducted using native and GRASS plugins in QGIS software (QGIS Development Team, 2024; GRASS Development Team, 2024), which do not permit specification of spatial scale for analysis. The evaluated metrics include the roughness index, total curvature, maximum curvature, absolute minimum curvature, curvedness index, unsphericity, and standard deviations of slope, profile curvature, plan curvature, tangential curvature, difference curvature, and mean curvature (Shary, 1995; Florinsky, 2017). Other captions follow **Fig. S2**.

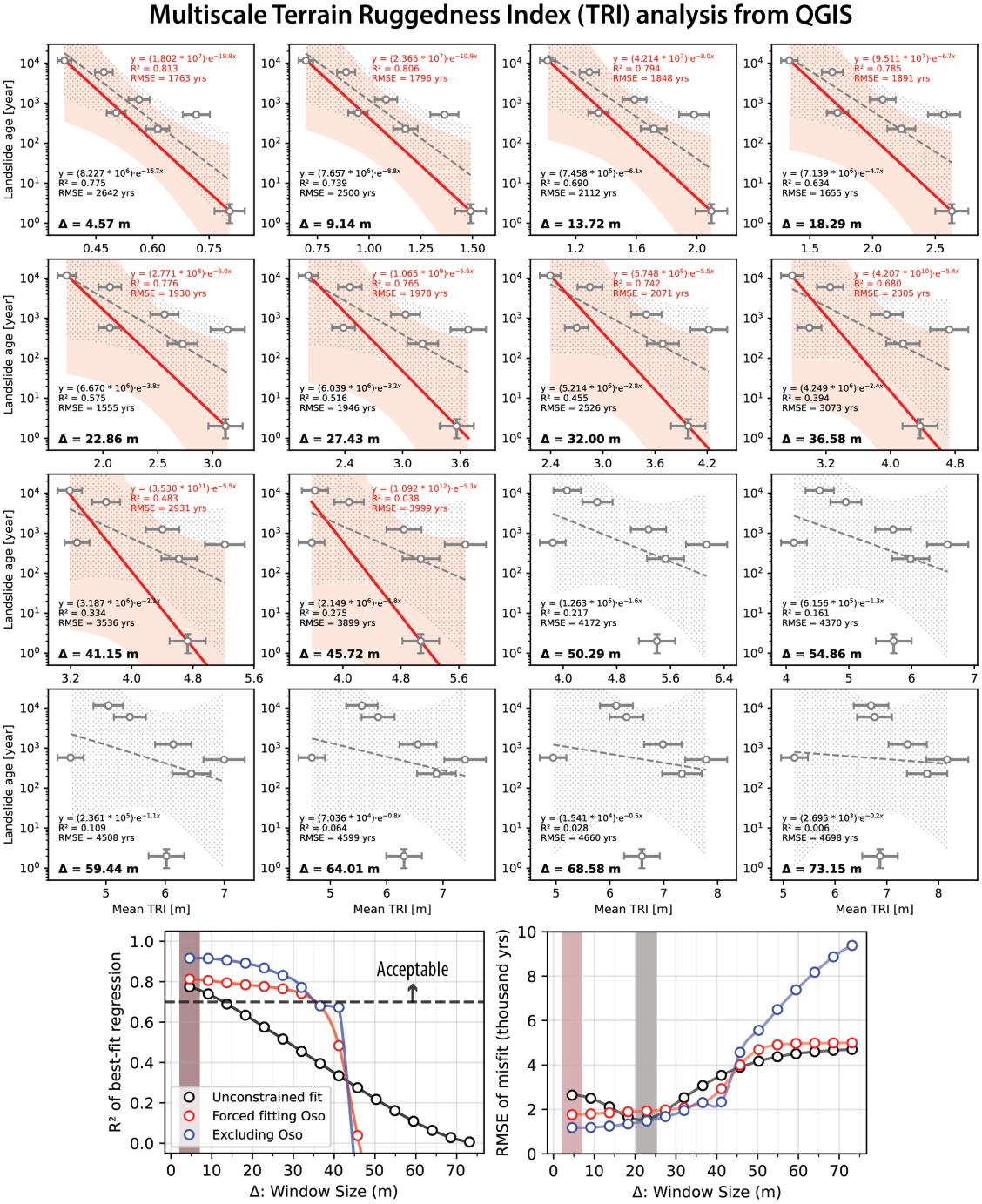

Figure S9: Evaluation of the Terrain Ruggedness Index (TRI) (Riley et al., 1999) for age of landslide deposits based on surface complexity, utilizing data from Booth et al. (2017) (**Fig. 3** and **Fig. S1**). This analysis utilized GRASS plugins in QGIS software, allowing for multiscale topographic complexity assessment. The evaluated spatial scale (window size Δ) ranges from 5 to 80 grids, corresponding to 15 feet (~4.57 m) to 240 feet (~73.15 m) with an input DTM featuring 3 feet (~0.9144 m) grid spacing. Other captions follow **Fig. S2**.

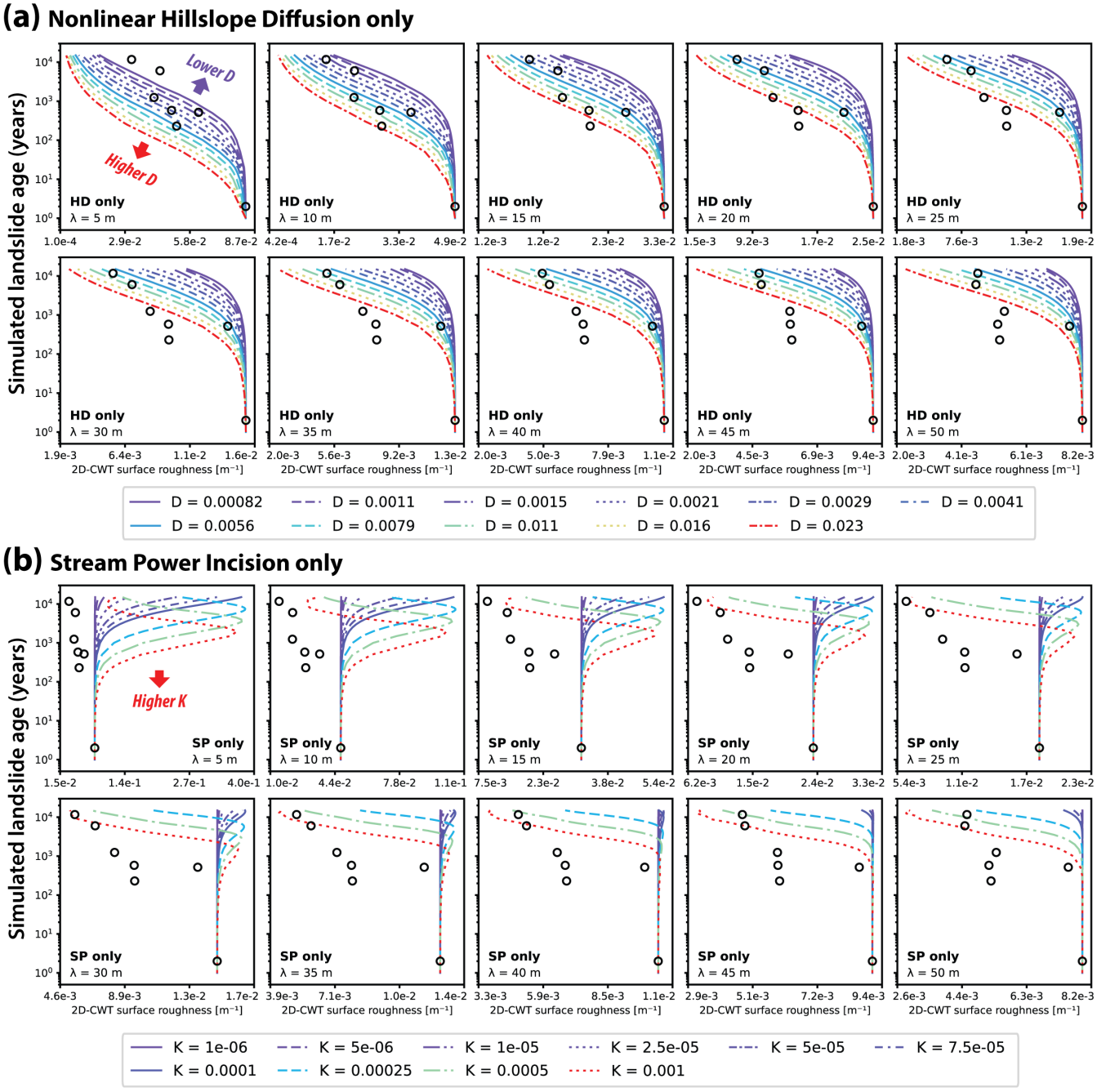

Figure S10: Changes in mean 2D-CWT surface complexity measures for the simulated landscape of the 2014 Oso landslide over a 15,000-year period, predicted by models of nonlinear hillslope diffusion (**a**) and stream power incision (**b**) in *Landlab_simulation.ipynb*, with varying hillslope diffusivity (D in m^2 yr^{-1}) and channel erodibility (K in $m^{0.5}$ yr^{-1}). Black circles represent real-world data from the seven dated landslide measurements in the North Fork Stillaguamish River valley (**Fig. 3a**).

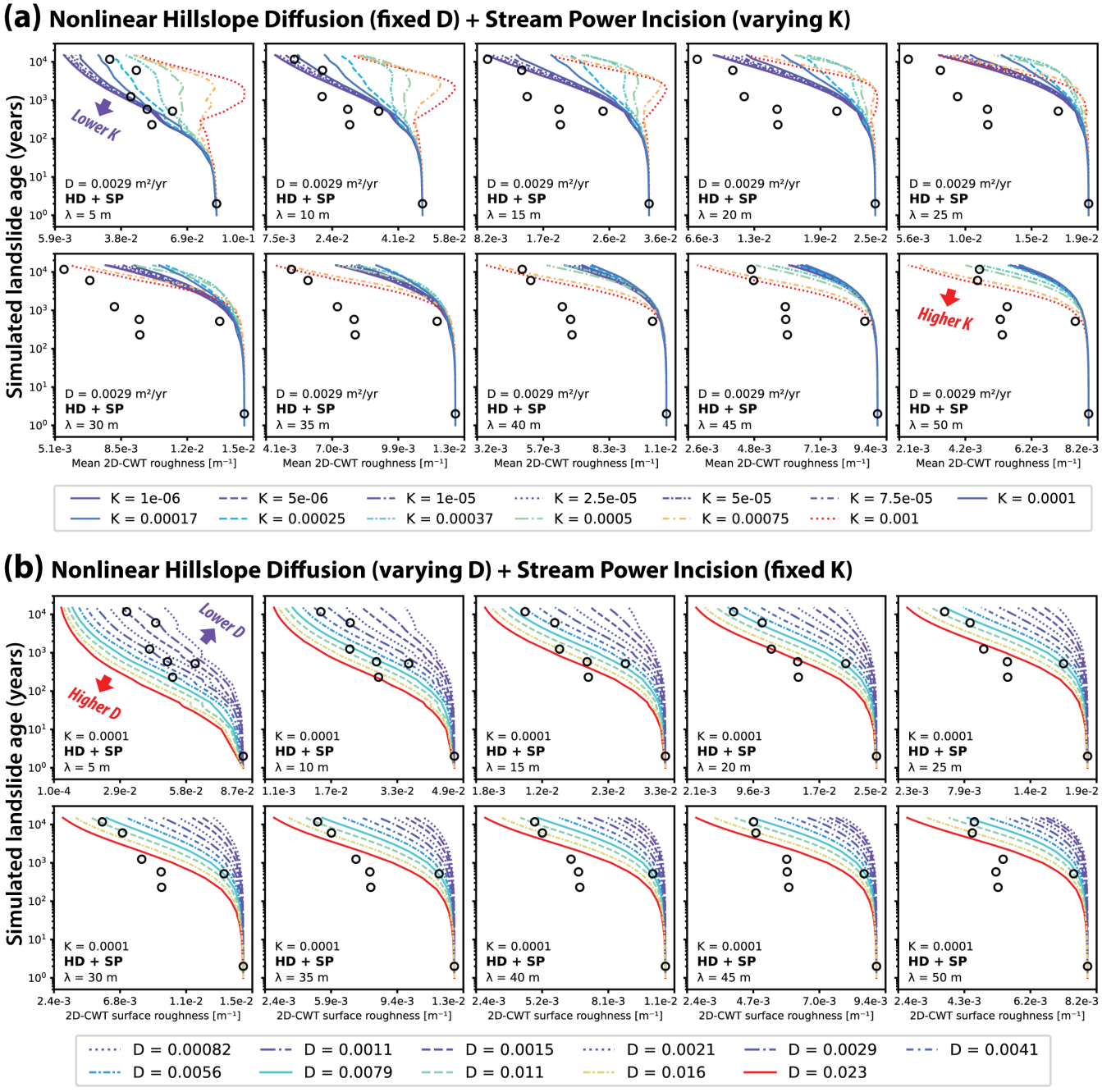

Figure S11: Changes in mean 2D-CWT surface complexity measures for the simulated landscape of the 2014 Oso landslide over a 15,000-year period, predicted by coupled models of nonlinear hillslope diffusion and stream power incision in *Landlab_simulation.ipynb*. (**a**) Simulations with a fixed $D = 0.0029$ m^2 yr^{-1} and varying channel erodibility (K in m$^{0.5}$ yr^{-1}). (**b**) Simulations with a fixed = 0.0001 m$^{0.5}$ yr^{-1} and varying D in m^2 yr^{-1}. Black circles represent real-world data from the seven dated landslide measurements in the North Fork Stillaguamish River valley (**Fig. 3a**).

References

Berti, M., Corsini, A., and Daehne, A.: Comparative analysis of surface roughness algorithms for the identification of active landslides, Geomorphology, 182, 1-18, https://doi.org/10.1016/j.geomorph.2012.10.022, 2013.

Booth, A. M., Roering, J. J., and Perron, J. T.: Automated landslide mapping using spectral analysis and high-resolution topographic data: Puget Sound lowlands, Washington, and Portland Hills, Oregon, Geomorphology, 109, 132-147, https://doi.org/10.1016/j.geomorph.2009.02.027, 2009.

Booth, A. M., LaHusen, S. R., Duvall, A. R., and Montgomery, D. R.: Holocene history of deep-seated landsliding in the North Fork Stillaguamish River valley from surface roughness analysis, radiocarbon dating, and numerical landscape evolution modeling, Journal of Geophysical Research: Earth Surface, 122, 456-472, https://doi.org/10.1002/2016JF003934, 2017.

Du Preez, C.: A new arc–chord ratio (ACR) rugosity index for quantifying three-dimensional landscape structural complexity, Landscape Ecology, 30, 181-192, 10.1007/s10980-014-0118-8, 2015.

Florinsky, I. V.: An illustrated introduction to general geomorphometry, Progress in Physical Geography: Earth and Environment, 41, 723-752, 10.1177/0309133317733667, 2017.

GRASS Development Team: Geographic Resources Analysis Support System (GRASS GIS) Software (8.2), Open Source Geospatial Foundation [code], https://doi.org/10.5281/zenodo.5176030, 2024.

Jenness, J. S.: Calculating landscape surface area from digital elevation models, Wildlife Society Bulletin, 32, 829-839, https://doi.org/10.2193/0091-7648(2004)032[0829:CLSAFD]2.0.CO;2, 2004.

Pardo-Igúzquiza, E. and Dowd, P. A.: Fractal Analysis of Karst Landscapes, Mathematical Geosciences, 52, 543-563, 10.1007/s11004-019-09803-x, 2020.

QGIS Development Team: QGIS Geographic Information System (3.38) [code], https://www.qgis.org, 2024.

Riley, S. J., DeGloria, S. D., and Elliot, R.: A Terrain Ruggedness Index that quantifies topographic heterogeneity, Intermountain Journal of Sciences, 5, 23-27, 1999.

Shary, P. A.: Land surface in gravity points classification by a complete system of curvatures, Mathematical Geology, 27, 373-390, 10.1007/BF02084608, 1995.

Weiss, A.: Topographic position and landforms analysis, Poster presentation, ESRI user conference, San Diego, CA,

Wen, R. and Sinding-Larsen, R.: Uncertainty in fractal dimension estimated from power spectra and variograms, Mathematical Geology, 29, 727-753, 10.1007/BF02768900, 1997.